Transactions, SMiRT-25
Charlotte, NC, USA, August 4-9, 2019
Division III - Computation, Simulation and Visualization

FLUID-STRUCTURE-INTERACTION ANALYSIS FOR A WATER HAMMER LOADED PIPING ELBOW

Ahti Oinonen[1]

[1] Research Scientist, VTT Technical Research Centre of Finland, Espoo, Finland (ahti.oinonen@vtt.fi)

ABSTRACT

This work is concerned with a numerical investigation of fluid-structure-interaction on a two-dimensional piping structure that is dynamically loaded. The solution procedure combines the method of characteristic for the fluid equations with the finite element method for beam structures. The fluid-structure-interaction is governed by junction coupling at the pipe elbow, and both friction and Poisson couplings are modelled as well. There is an application on solving the pressure, displacement and bending stress responses due to a water hammer event caused by a rapid valve closure combined with external harmonic loading. The studied structure involves a valve, tank and elbow that are described as boundary conditions. Results show that water hammer loading combined with the excitation force causes significantly increased displacements and higher stress peaks if the frequencies of the harmonic loading and the natural mode of the structure coincide.

INTRODUCTION

According to nuclear power plant regulations and standards (U.S. Nuclear Regulatory Commission 1984; ASME 2015), dynamic stresses caused by both the Water Hammer (WH) phenomenon and mechanical loading need to be considered during design of the safety-classified piping structures. These dynamically induced forces simultaneously affect fluid and pipe components. If the natural frequency of the piping structure coincides with the frequency of excitation loading, a condition of resonant vibration could occur, even with damaging consequences.

Dynamic loads are characterized as local and distributed forces. The local forces result in structural motion that affects and induces stress waves in the fluid. They typically act at the points of discontinuity of piping such as at elbows and at valves. This interaction is referred as junction coupling (Lavooij and Tijsseling, 1991). In contrast, the distributed forces act along piping. Axial stress waves in the pipe shell are caused by high-pressure gradients that expand and contract the pipe. In addition, the distributed forces due to fluid friction affect along piping. These two latter interactions are called as Poisson and friction couplings (Lavooij and Tijsseling, 1991).

WH affected flow in piping systems can be idealized as a system of the continuity and momentum equations (Ghidaoui et al., 2005). The applicable combined solution procedure for Fluid-Structure-Interaction (FSI) analyses of WH loaded piping consists of applications of the Method of Characteristics (MOC) to fluid equations and the Finite Element Method (FEM) to structural analysis (Lavooij and Tijsseling, 1991; Heinsbroek, 1997; Ahmadi and Keramat, 2010). The MOC solver processes both flow and pressure, which is used as input data for generating the load vector for the piping structure. Possibly affecting external forces are included into a definition of the load vector. The Newmark scheme is directly applied to the integration of the structural equations of piping. At the pipe ends, relations between pressure and flow are governed by well-defined Boundary Conditions (BCs) that are also specified at the elbow

locations of piping. Thus, junctions coupling is modelled in terms of BCs, and both Poisson and friction couplings are included in the formulation of the governing differential equations that are solved with the MOC.

This work is concerned with a computer implementation and numerical investigation of the FSI on a two-dimensional piping structure that is subjected dynamic loading conditions. Short descriptions of the solution methods for piping responses due to transient flow and related structural loads are first presented. The chosen benchmark structure represents the piping configuration previously studied by Lavooij and Tijsseling (1991). In this study, there is harmonic loading demonstrating external machine excitation as well. Rayleigh damping is included in the computations. The flow behaviour is considered as one-dimensional and isothermal and the piping structure is modelled using Euler-Bernoulli beam elements. The scope of this work is to investigate the FSI involving the junction, friction and Poisson couplings on the model structure, which is subjected to both the WH event and harmonic excitation force. Influences of these loadings on the dynamic pressure, longitudinal displacement and bending stress are assessed as well.

METHODS

The fundamental equations can be applied in calculations of input data for FSI computations with the combined MOC-FEM procedure. Pressure solved with the MOC is used for generating the load vector for the piping structure. These forces affecting the piping filled with fluid cause lateral motion that can be solved with the FEM using Euler-Bernoulli beam elements. With stability and accuracy in the mind, the dynamic problem in terms of the equation of motion is solved with the Newmark scheme.

Fundamental Equations

The peak pressure caused by the WH event can be calculated from the equation derived by Frizell (1898)

$$\Delta p = \rho_f c_f \Delta \dot{u}_x, \tag{1}$$

where Δp is the difference in the pressure magnitude of the wave, ρ_f is the density of the fluid and $\Delta \dot{u}_x$ is the difference in the velocity of the fluid along the axial coordinate of the pipe component. For Equation (1), the wave speed c_f of the WH, i.e. the speed of sound in the fluid can be calculated from (Tijsseling, 1996; Ghidaoui et al., 2005)

$$c_f^2 = \frac{k_f}{\rho_f}\left(1 + \frac{d k_f (1-\nu^2)}{sE}\right)^{-1}, \tag{2}$$

where the bulk modulus of elasticity of the fluid is denoted by k_f, and for piping E is the Young's modulus, ν is the Poisson ratio and s is the piping wall thickness whereas the inside diameter is denoted by d. The principal period of the WH waves can be calculated by assuming constant distribution of acoustic pressure,

$$T_{wh} = 4L/c_f, \tag{3}$$

which holds for pipes of the length L with one end closed and other end open (Au-Yang, 2001).

Unsteady flow of liquid in closed piping can be modelled with the classical Equation (4) of conservation of mass, i.e. the continuity equation and with Equation (5) of conservation of linear momentum (Lavooij and Tijsseling, 1991; Ghidaoui et al., 2005)

$$\frac{g}{c_f^2}\frac{\partial h}{\partial t}+\frac{\partial q}{\partial x}-\frac{2\nu}{E}\frac{\partial \sigma_x}{\partial t}=0, \tag{4}$$

$$\frac{\partial q}{\partial t}+g\frac{\partial h}{\partial x}+\frac{f}{2d}q_r|q_r|=0, \tag{5}$$

where h denotes the hydraulic head, t time, x the spatial coordinate along piping, g the gravitational acceleration and σ_x the axial stress, respectively. In Equation (5), the relative velocity of fluid is calculated from the fluid velocity q and structural motion of the pipe, $q_r = q - \dot{u}_x$. The Darcy friction constant f weights the last term of Equation (5). It is noted that the last term of Equation (4) does not affect the solution if the Poisson coupling is excluded.

Method of Characteristics

The MOC is based on reducing a Partial Differential Equation (PDE) to a family of ordinary differential equations along the directions that allow the numerical solution to be integrated from essential initial data given on a suitable hypersurface. These equations provide a technique to calculate the h and q rates at any arbitrary point at the node i if the conditions at the nodes i and $i+1$ or at i and $i-1$ are known (Griffiths et al., 2015). For the PDE of the form of Equations (4) and (5), integral curves for the vector field associated with the PDE are first obtained and an integral surface as a union of these characteristic curves is formed to solve the problem (Griffiths et al., 2015).

The system of the WH equations is hyperbolic, since the characteristic directions are distinct and real. The hyperbolic set is transformed to sets of ordinary differential equations, which are denoted by C^+ and C^- (Griffiths et al., 2015). To obtain finite difference formulas, the piping length is divided into equal Δx, which can be calculated from the selected time step Δt for the MOC solution (Lavooij and Tijsseling, 1991),

$$\Delta x = c_f \Delta t. \tag{6}$$

The compatibility Equations (4) and (5) can be rewritten as (Lavooij and Tijsseling, 1991)

$$C^+: \quad \frac{c_f}{g}\frac{\partial q}{\partial t}+\frac{\partial h}{\partial t}+f\frac{q_r|q_r|}{2gd}-\frac{2\nu c_f^2}{gE}\frac{\partial \sigma_x}{\partial t}=0, \tag{7}$$

$$C^-: \quad \frac{c_f}{g}\frac{\partial q}{\partial t}-\frac{\partial h}{\partial t}+f\frac{q_r|q_r|}{2gd}+\frac{2\nu c_f^2}{gE}\frac{\partial \sigma_x}{\partial t}=0, \tag{8}$$

where the derivative $\partial\sigma_x/\partial t$ is here estimated from the difference $\sigma_{i-1/2}^{t+1} - \sigma_{i-1/2}^{t}$. Equation (7) is applied along the characteristic line equation $dx = c_f dt$ and Equation (8) along $-dx$, correspondingly. Substituting the previous equalities to the finite difference scheme results in the equalities that can be solved for h and q for each $t + \Delta t$ (Lavooij and Tijsseling, 1991)

$$C^+: \quad h_i^{t+\Delta t} - h_{i-1}^t = \frac{-c}{g}\left(q_i^{t+\Delta t} - q_{i-1}^t\right) - \frac{f\Delta x}{2gd}q_{i-1}^t|q_{i-1}^t| + \frac{2\nu c_f^2}{gE}\frac{\partial \sigma_x}{\partial t}, \tag{9}$$

$$C^-: \quad h_i^{t+\Delta t} - h_{i+1}^t = \frac{c}{g}\left(q_i^{t+\Delta t} - q_{i+1}^t\right) + \frac{f\Delta x}{2gd}q_{i+1}^t|q_{i+1}^t| + \frac{2\nu c_f^2}{gE}\frac{\partial \sigma_x}{\partial t}, \tag{10}$$

Finite Element Method

With the FEM, the piping is divided into beam elements, and the structural equations are transformed to algebraic equations (Cook et al., 2002). Discretizing pipe geometry into beam elements yields the solution that is valid for the whole piping assembly. Euler-Bernoulli beam elements have been shown as adequate for practical piping analyses involving FSI (Heinsbroek, 1997). On each element, displacements and the test function are interpolated using the shape functions and corresponding nodal values. The global stiffness and mass matrices and load vector are obtained by assembling the individual element contributions. For FSI, a common valued Δx for both the MOC and FEM is assumed as a good choice.

Boundary Conditions

For solutions with the MOC, relations between the head and discharge are required at each end of the piping member. The BCs at pipe ends consist of constant or variable pressure or flow due to valve operations. The BCs for tanks with the constant head h_{st} are

$$h = h_{st} \text{ and } u_x = 0, \tag{11}$$

and for closed valves rigidly supported to the ground

$$q = 0 \text{ and } u_x = 0. \tag{12}$$

For piping elbows, the structural force BC is required due to junction coupling of piping with the local flow area A_f (Ahmadi and Keramat, 2010),

$$f_{i-1} = \left(A_f h\right)_{i-1} \rho_f g \text{ and } f_{i+1} = \left(A_f h\right)_{i+1} \rho_f g, \tag{13}$$

and the elbows are also simplified as grid points with the zero control volume resulting in the following BCs (Lavooij and Tijsseling, 1991),

$$h_{i-1} = h_{i+1} \text{ and } \left(A_f q\right)_{i-1} - \left(A_f q\right)_{i+1} = \left(A_f \dot{u}_x\right)_{i-1} - \left(A_f \dot{u}_x\right)_{i+1}. \tag{14}$$

Equation of Motion

The second order differential equation of motion is of the form (Cook et al., 2002)

$$M\ddot{u} + C\dot{u} + Ku = f(x,t), \tag{15}$$

where M and K are the mass and stiffness matrices. To complete the definition of the initial value problem, initial conditions for the displacement u and velocity $\dot{u}$ are prescribed.

The damping matrix is obtained from

$$C = \mu M + \lambda K, \tag{16}$$

where μ and λ are the mass and stiffness proportional Rayleigh damping coefficients. The time-dependent vector $f(x,t)$ contains load data for each structural node and the inertia of piping is represented by M. The structural Equation (15) is solved at time increments specified by Δt for the total time T with the Newmark $\beta = 1/4$ solution scheme that corresponds to the trapezoidal rule (Cook et al., 2002).

RESULTS

First, the model structure is introduced. Results corresponding to the case previously published by Lavooij and Tijsseling (1991) are solved for validation of the present computer implementation. Dynamic pressure $p(t)$, displacements $u(t)$ and bending stress $\sigma_b(t)$ are computed both with and without harmonic excitation loading. All analyses are solved with $\Delta t = 10^{-5}$ s and Δx according to Equation (6).

Model Structure

The layout of the piping structure with the valve, tank and elbow is shown in Figure 1. The dimensions and material data are listed in Table 1 and loading related data in Table 2, respectively. The WH shock direction is to the right. In addition, there is external excitation loading of the harmonic form

$$f_x(x,t) = F_0 \sin(\omega t). \tag{17}$$

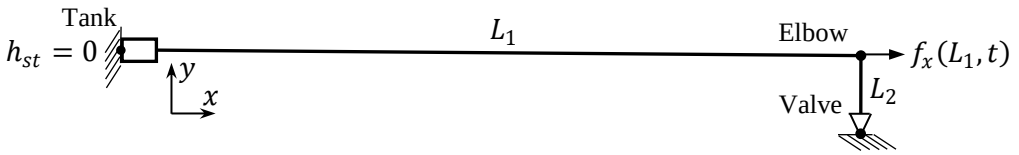

Figure 1. Configuration of the idealized piping structure with the fixed valve and tank.

Table 1: Dimension and material data according to the case study in Lavooij and Tijsseling (1991).

Wall thickness of the pipe, s (mm)	6.35
Outer diameter of the pipe, D (mm)	219
Length of the horizontal pipe member, L_1 (m)	310
Length of the vertical pipe member, L_2 (m)	20
Young's modulus, E (GPa)	210
Density of the pipe material, ρ_p (kg/m^3)	7900
Density of water, ρ_f (kg/m^3)	880
Damping ratio, ζ	0.05

Table 2: Loading data for the piping model.

Initial fluid velocity along piping, $q(x, 0)$ (m/s)	4
Time period of valve closure, Δt_v (ms)	8.7
Excitation force amplitude, F_0 (kN)	175
Excitation frequency, ω (rad/s)	5.7

Fluid Structure Interaction on the Model Structure

The dynamic stresses and horizontal displacement responses at the elbow location are presented in Figure 2 that includes the results computed involving both the friction and junction couplings, and with all three types of couplings considered in this work. Figure 5 shows the displacements at the right end of this model. Figure 3 shows the corresponding results for the case involving the three couplings and external harmonic excitation load. The results have been computed with WH and coinciding external excitation, with WH and contrary external excitation and with WH excluding harmonic excitation. In Figure 4, there are comparisons of the dynamic bending stress σ_b at the valve and tank locations.

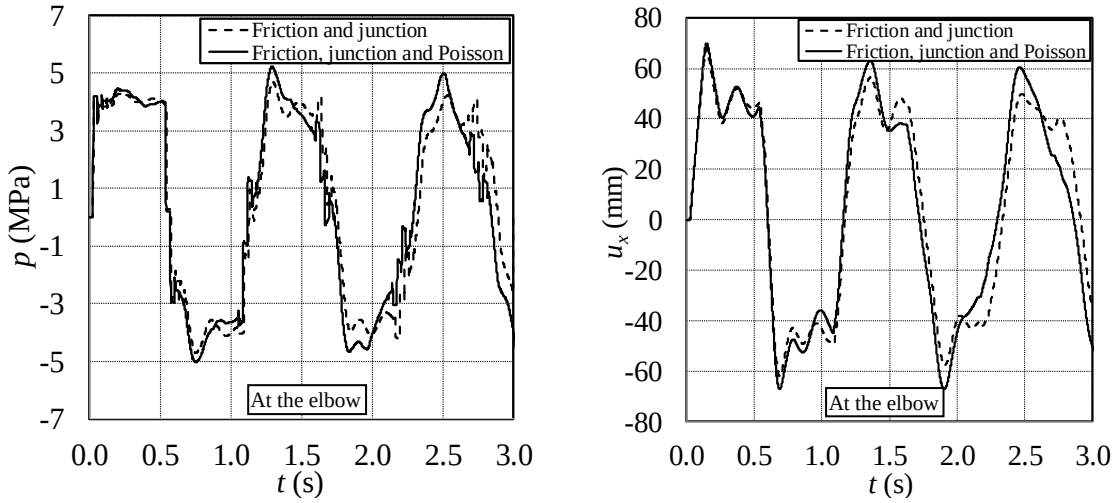

Figure 2. Comparison of the dynamic pressure and horizontal displacements at the elbow location of piping computed with the junction and friction, and with the junction, friction and Poisson couplings.

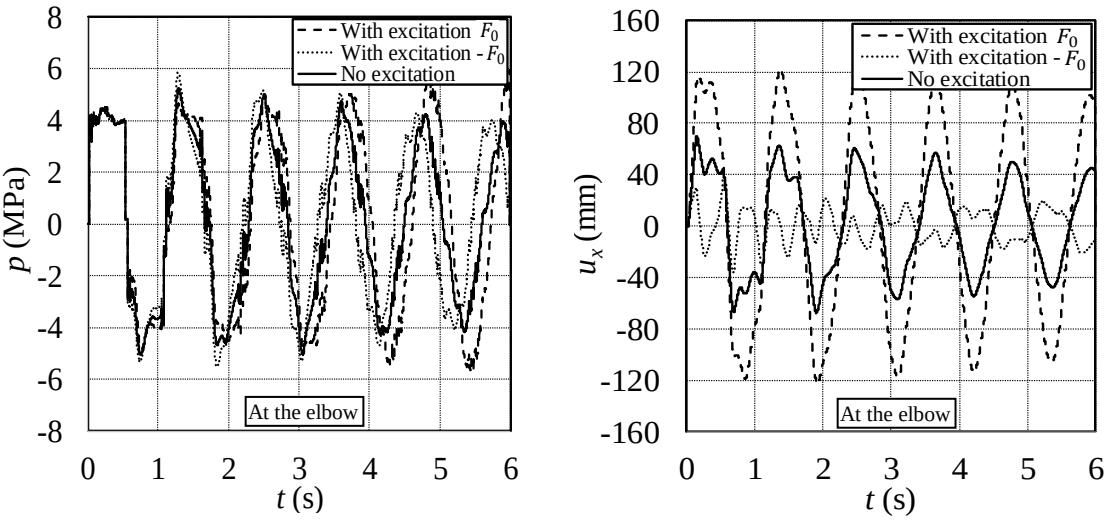

Figure 3. Comparison of the dynamic pressure and horizontal displacement results at the elbow location.

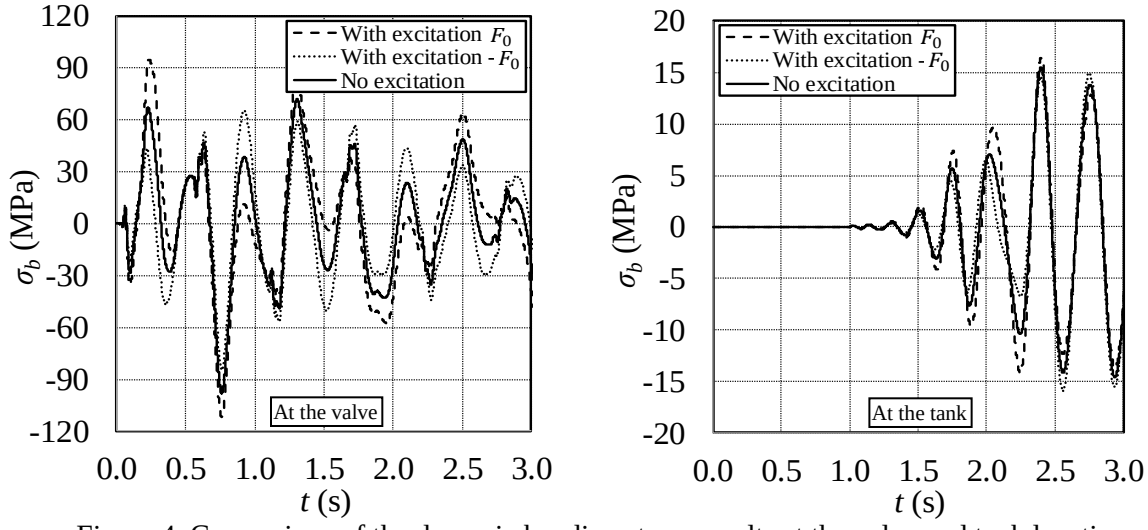

Figure 4. Comparison of the dynamic bending stress results at the valve and tank locations.

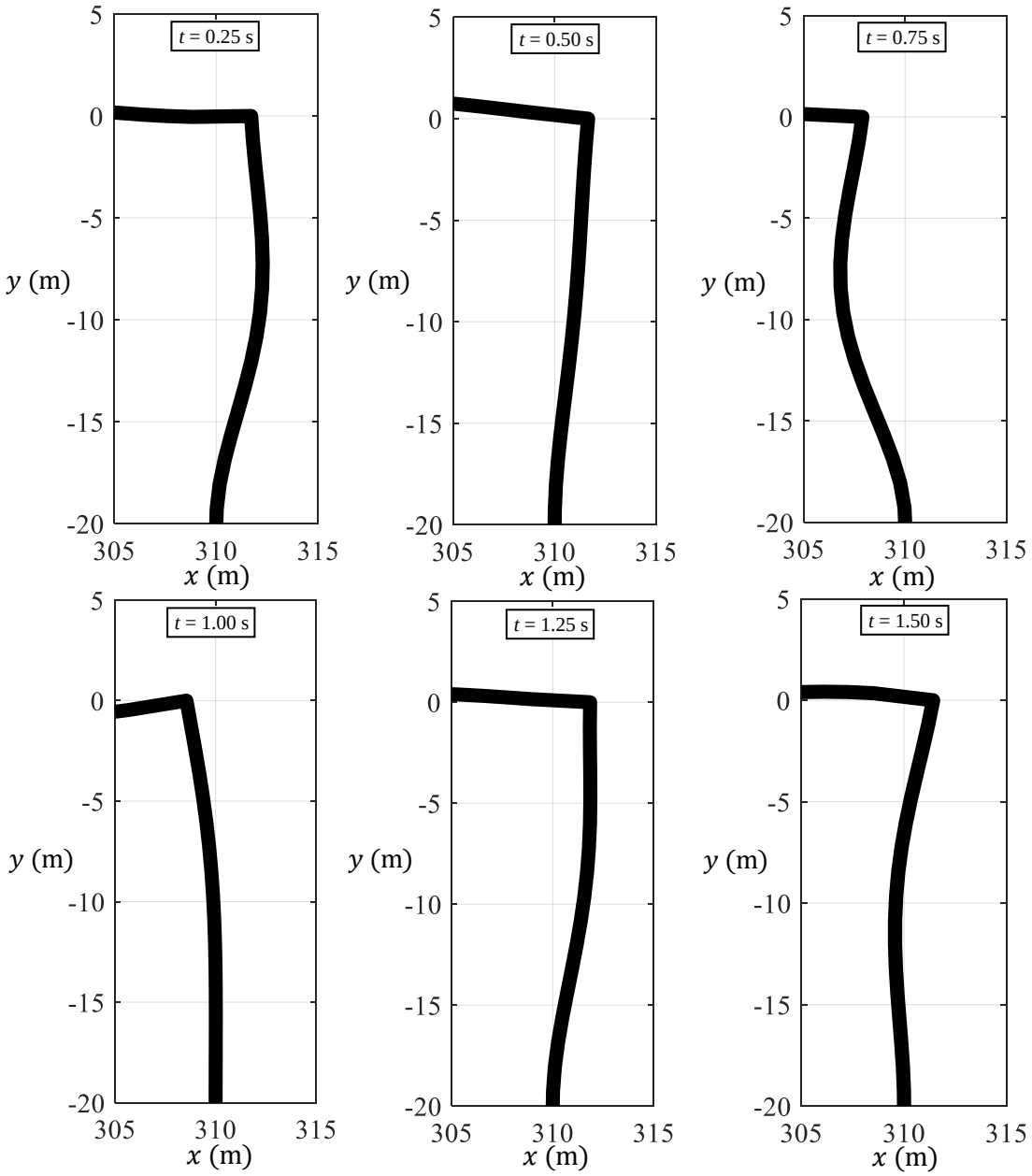

Figure 5. Dynamic displacement modes of the right end of piping at the 0.25 s intervals until t = 1.5 s for the case without excitation and with three couplings. Displacements are exaggerated by the factor of 40.

DISCUSSION

Lavooij and Tijsseling (1991) state that significant FSI effects for the studied geometry can be expected, since $T_{eff} < T_f < 4L/c_f$. In this inequality, T_{eff} denotes the effective closure time of the valve, T_f states the eigenperiod of the piping structure with the length L. Based on that, FSI effects on the structural response increase both when L increases and when T_{eff} decreases. With reference to Equation (3), the main scale of WH waves is approximately $T_{wh} = 1.1$ s, which can also be concluded from Figure 2. For harmonic excitation loading, ω was chosen to coincide with the frequency calculated from ${T_{wh}}^{-1}$. According to Lavooij and Tijsseling (1991), the natural mode of the structure is governed by the axial motion of the horizontal member.

In Figure 2, the results computed for validation purposes show a good agreement with the corresponding reference plots published by Lavooij and Tijsseling (1991). Further results computed with the implemented MOC-FEM procedure are presented in Figures 3 - 5. The applied excitation load with F_0 causes double the values of longitudinal displacement peaks at the elbow location as compared to the corresponding cases computed without excitation or with the opposite direction of the excitation force amplitude, $-F_0$. Additionally, the peak values of $p(t)$ increase due to coinciding $F_0\sin(\omega t)$ as can be observed from Figure 3. Furthermore, the resulted peak values of σ_b at the outer pipe radius location are considerably higher with the coincident F_0. The magnitude of F_0 was chosen to correspond to the respective maximum peak force attained at the elbow location caused by the WH event.

The peak pressure caused by the WH event can be approximated from Figure 1. Hence, $\Delta p \approx 4.4$ MPa after the first fluctuation and the maximum attained $\Delta p \approx 5.1$ MPa with considering all three couplings. The corresponding result as calculated from Equation (1) is $\Delta p \approx 4.2$ MPa. However, the more complex results presented in Figures 4 and 5 would be very difficult to even approximately access with the simpler approaches, since dynamical effects govern the solutions. At the valve location, the maximum peak value of $|\sigma_b| \approx 98$ MPa is attained if there is no excitation loading and with coinciding excitation $|\sigma_b| \approx 112$ MPa, respectively. In contrast, the maximum $|\sigma_b|$ at the tank location is relatively low. Furthermore, the exaggerated displacement modes of the right end of piping at the 0.25 s time intervals for the case without excitation and involving the junction, friction and Poisson couplings illustrate the dynamic behaviour of the structure subjected to the WH event.

CONCLUSIONS

FSI was numerically investigated on a two-dimensional dynamically loaded piping structure with the combined MOC-FEM procedure including three types of coupling. The studied piping system was modelled as a structural frame composed of Euler-Bernoulli beam elements. Rayleigh damping was applied to filtering out high frequency modes. It can be concluded that the FSI effects on the structural responses are significant due to both the relatively high dynamic loads and geometry of the model structure. In the result plots, this can be seen as the relatively high displacements and bending stress peaks. With the studied FSI method, bending stress responses can be solved with a good accuracy. The combined MOC-FEM procedure for solving the FSI problem can be considered as very suitable and efficient for computations of the structural responses due to WH events and external harmonic loads. The presented numerical results can be applied by engineers in the selection of analysis methods for dynamic piping problems and in their assessments to find when FSI is significant.

NOMENCLATURE

c_f	Wave speed in the fluid
f	Darcy friction coefficient
$f(x,t)$	Force vector
g	Gravitational acceleration
h	Hydraulic head
h_{st}	Constant tank head
i	Node number
k_f	Bulk modulus of elasticity of the fluid
p	Pressure magnitude
q, q_r	Velocity and relative velocity of the fluid
s	Thickness of the pipe wall
t	Time
Δt	Time step

Δt_p	Pressure shock duration
u	Displacement vector
x, y	Spatial coordinates
Δx	Spacing of spatial discretization for both the MOC and FEM
A_f	Flow area
C	Damping matrix
D	Outer diameter of the pipe
C^+, C^-	Sets of characteristic lines related to the wave velocity
E	Young's modulus
F_0	Force amplitude
K	Stiffness matrix
L	Piping length
M	Mass matrix
T	Analysis period
T_{eff}	Effective closure time of the valve
T_f	Eigenperiod of the structure
T_v	Time period of valve closure
T_{wh}	Main scale of WH waves
β	Parameter of the Newmark method
ζ	Damping ratio
σ_b, σ_x	Bending and axial stresses
λ, μ	Stiffness and mass proportional damping coefficients
ν	Poisson's ratio
ρ_f, ρ_w	Densities of the fluid and pipe material
ω	Angular frequency of the harmonic excitation load

REFERENCES

Ahmadi, A. and Keramat, A. (2010). "Investigation of fluid–structure interaction with various types of junction coupling" *Journal of Fluids and Structures*, 26 1123-1141.

ASME Boiler & Pressure Vessel Code (2015). "Rules for Construction of Nuclear Facility Components", *Nonmandatory Appendix W - Article W-4000 Summaries of other damage mechanicms*, The American Society of Mechanical Engineers.

Au-Yang, M. K. (2001). *Flow-Induced Vibration of Power and Process Plant Components*, ASME Press.

Cook, R. D., Malkus, D. S., Plesha, M. E. and Witt, R. J. (2002). *Concepts and Applications of Finite Element Analysis, 4th ed*., John Wiley & Sons.

Frizell, J. P. (1898). "Pressures Resulting From Changes of Velocity of Water in Pipes", *Transactions of the American Society of Civil Engineers*, XXXIX 1-7.

Ghidaoui, M. S, Zhao, M, McInnis, D. A, Axworthy, D. H. (2005). "A Review of Water Hammer Theory and Practice", *Applied Mechanics Reviews*, 58 49-75.

Griffiths, D. F., Dold, J. W. and Silvester, D. J. (2015). *Essential Partial Differential Equations, Analytical and Computational Aspects*, Springer.

Heinsbroek, A. G. T. J. (1997). "Fluid-structure interaction in non-rigid pipeline systems", *Nuclear Engineering and Design*, 172 123-135.

Lavooij, C. S. W. and Tijsseling, A. S. (1991). "Fluid-structure interaction in liquid-filled piping systems", *Journal of Fluids and Structures*, 5 573-595.

Tijsseling, A. S. (1996) "Fluid-structure interaction in liquid-filled piping systems: A review" *Journal of Fluids and Structures*, 10 109-146.

U.S. Nuclear Regulatory Commission (1984). "Evaluation of water hammer occurrence in nuclear power plants", *NUREG-0927, Rev. 1*, Washington, D.C.